

Detection of H α Emission from the Magellanic Stream: Evidence for an Extended Gaseous Galactic Halo

Benjamin J. Weiner¹ and T. B. Williams¹

Department of Physics and Astronomy, Rutgers, The State University

Box 849, Piscataway, NJ 08855-0849

bweiner@physics.rutgers.edu, williams@physics.rutgers.edu

Rutgers Astrophysics Preprint No. 180

ABSTRACT

We have detected faint H α emission from several points along the Magellanic Stream, using the Rutgers Fabry–Perot Interferometer at the CTIO 1.5-m telescope. The sources of the emission are diffuse; at each observed position, there is no variation in intensity over the 7' field of the Fabry–Perot. At points on the leading edges of the H I clouds MS II, MS III, and MS IV, we detect H α emission of surface brightness 0.37 ± 0.02 Rayleighs, 0.21 ± 0.04 R, and 0.20 ± 0.02 R respectively, corresponding to emission measures of 1.0 to 0.5 cm⁻⁶ pc. We have observed several positions near the MS IV concentration, and find that the strongest emission is on the sharp leading-edge density gradient. There is less emission at points away from the gradient, and halfway between MS III and MS IV the H α surface brightness is < 0.04 R.

We attribute the H α emission at cloud leading edges to heating of the Stream clouds by ram pressure from ionized gas in the halo of the Galaxy. These observations suggest that ram pressure from halo gas plays a large role in stripping the Stream out of the Magellanic Clouds. They also suggest the presence of a relatively large density of gas, $n_{\text{H}} \sim 10^{-4}$ cm⁻³, in the Galactic halo at ~ 50 kpc radius, and far above the Galactic plane, $|b| \sim 80^\circ$. This implies that the Galaxy has a very large baryonic, gaseous extent, and supports models of Lyman- α and metal-line QSO absorption lines in which the absorption systems reside in extended galactic halos.

Subject headings: galaxies: Magellanic Clouds – Galaxy: corona of – Galaxy: halo of – quasars: absorption lines

¹Visiting Astronomer, Cerro Tololo Inter-American Observatory. CTIO is operated by AURA, Inc. under contract to the National Science Foundation.

1. Introduction

The Magellanic Stream is a long filament of H I clouds which stretches over 100° on the sky, trailing behind the Magellanic Clouds in their orbit around the Galaxy (Mathewson *et al.* 1974). Observations of the Stream at 21 cm wavelengths show that it is a chain of clouds, connected by lower-density gas; the clouds have been labeled MS I through MS VI by Mathewson *et al.* (1977). These clouds generally have a high-density concentration with a relatively sharp density gradient on the leading edge, where the leading edge is determined by the direction of the proper motion of the LMC (Jones *et al.* 1994). The Stream has no known stellar component (Recillas-Cruz 1982, Brück & Hawkins 1983, Mathewson *et al.* 1979); it has previously been detected only in the 21 cm H I line, and in absorption against a background galaxy (Songaila 1981, Lu *et al.* 1994). Hence, its distance is unknown, although its leading end, MS I, connects to the Magellanic Clouds and is presumably at 50–60 kpc; recent estimates for the distance of the tip, MS VI, range from 20 kpc (Moore & Davis 1994) to 60 kpc (Gardiner *et al.* 1994).

There are many candidate explanations for the origin of the Magellanic Stream; most invoke either tidal or ram-pressure forces to detach the Stream from the Clouds. In tidal models, the Stream is torn out of the Magellanic Clouds by gravitational tides variously attributed to: the Galaxy (*e.g.* Lin & Lynden-Bell 1977, Gardiner *et al.* 1994, Lin *et al.* 1995), an encounter between the LMC and SMC (Murai & Fujimoto 1980), or an encounter with M31 (Shuter 1992). A weakness of tidal models is that stars should also be affected by tides, yet no stars appear to be associated with the Stream.

In ram-pressure models, the Stream is swept out of the Magellanic Clouds by gas postulated to exist in the Galactic halo, such as a diffuse ionized corona (*e.g.* Bregman 1979, Meurer *et al.* 1985, Sofue 1994), or an extended ionized disk and halo (Moore & Davis 1994). These models have had to invoke halo gas *ad hoc*. Another difficulty is that the timescale for a stripping instability to develop may be very long for reasonable halo gas densities (Bregman 1979). It is clear that these scenarios for the formation of the Stream are highly dependent on unknowns such as the mass and extent of the Galactic halo and the putative ionized Galactic corona. Conversely, the Stream can be a probe of these unknowns.

We report here the results of high-sensitivity observations of H α emission from the Magellanic Stream, using the Rutgers Imaging Fabry–Perot interferometer (RFP). The Fabry–Perot simultaneously provides spectral coverage over a short wavelength interval, and a large collecting area, making it well suited to search for faint diffuse emission lines (Williams 1994).

In section 2 we describe the observations and data reduction. In section 3 we summarize the results and H α detections, and show that the emission is associated with cloud leading edges. In section 4, we consider possible sources for the emission and show that the most plausible source is heating of the Stream gas by ram pressure, arising as the clouds of the Stream collide with diffuse gas in the Galactic halo. This diffuse gas is probably at the virial temperature of the halo,

$T \sim 2 \times 10^6$ °K, implying the existence of a tenuous, hot ionized Galactic corona.

2. Observations

We used the RFP at the f/7.5 Cassegrain focus of the CTIO 1.5-m telescope. The etalon used has resolution $\sigma = 15 \text{ km s}^{-1}$, 0.75 \AA FWHM at $\text{H}\alpha$, and the free spectral range is 22 \AA . The detector was the Tek 1024 #2 CCD, binned 2×2 , giving $1.94''$ pixels; the gain was 1.7 electrons/ADU and the read noise was 4.9 electrons. The field of view of the RFP is $7'$ in diameter; there is a 5.5 \AA gradient in wavelength from center to edge of the field. We used a blocking filter of central wavelength 6560 \AA and FWHM 12 \AA , which ensures that only one Fabry–Perot order is imaged. The images are flat-fielded using IRAF.²

The observations were made on the nights of 12–16 August, 1994. Table 1 lists the object fields observed and summarizes the results. The individual exposures were 15 minutes each; in order to achieve accurate sky subtraction, we took exposures of sky fields 8° – 15° away from each object, chosen to be in regions free of high-velocity H I. Generally we sequenced exposures so that each object spectrum has its corresponding sky exposure obtained immediately before or after. Individual exposures on the same field were offset in different directions by $30''$ to avoid any spatial structure which might mimic an emission line. Exposures of a hydrogen lamp were taken every hour for wavelength calibration. The weather was excellent; all five nights were photometric. The flux calibration was derived by observing the planetary nebula NGC 6302 (Acker *et al.* 1993), scanning the $\text{H}\alpha$ emission line.

Since the center-to-edge gradient is considerably larger than the resolution of the etalon, any diffuse emission line which fills the field will appear as a ring around the optical axis of the etalon. We divide the image into circular annuli with width corresponding to 0.1 \AA , and estimate the flux within each annulus, to obtain a 5 \AA long section of the spectrum of the field. Each annulus contains the same number of pixels, due to the parabolic variation of wavelength with radius.

We estimate the average flux per pixel in each annulus using the biweight statistic (Beers *et al.* 1990); the biweight gives very little weight to outliers, which effectively clips stars and cosmic rays. We derive an error estimate from the biweight scale, a robust analog of the standard deviation. This estimated error, derived directly from the dispersion among the pixels in each sample, is consistent with that expected from the read noise and photon statistics.

We pair each object-field spectrum with a sky-field spectrum and subtract to isolate the object contribution. There is generally an offset in the continuum due to temporal variations, differences in airmass, and scattered moonlight, so we subtract a constant continuum level, determined by

²IRAF is distributed by NOAO, which is operated by AURA Inc., under contract to the NSF.

taking the biweight of a region of the spectrum away from any object or atmospheric emission lines. Figure 1 shows an example: the spectra from one pair of object and sky exposures for the MS II A field, and the residual object spectrum, with the signature of an emission line. The observed wavelength agrees with the LSR velocity of the H I observed by Morras (1985). The strong feature at 6563 Å is the geocoronal H α line, demonstrating the sensitivity of the Fabry-Perot, since this is a rather weak atmospheric feature (Osterbrock & Martel 1992). The emission from MS II is visible at 6560 Å. The height of the peak corresponds to 2.5 electrons per pixel; the ring signature of the MS II emission line is actually visible in the raw object-field CCD frame. The intensity of the H α line from MS II A is 0.37 Rayleighs (1 Rayleigh = 10^6 photons cm $^{-2}$ s $^{-1}$ sr $^{-1}$), or an emission measure (EM) of 1.0 cm $^{-6}$ pc, if the gas is at 10 4 °K. The total combined spectrum of MS II A, shown in Figure 2(a), is composed of six object–sky pairs like that shown in Figure 1(c).

3. Results

For each object field observed, we combined the object-minus-sky pairs, first subtracting a continuum from each pair. In Figure 2(a-c), we present the total combined spectra for fields MS II A, MS III, and MS IV C, which are located at the leading edges of H I density concentrations within each cloud. We also plot a LOWESS fit to the data; LOWESS (locally weighted scatterplot smoothing) is a robust smoothing algorithm (Cleveland & McGill 1984). In each of the three fields, a H α emission line is visible, at a velocity which agrees with the H I velocity from observations at 21 cm. The intensities, derived from fitting Voigt profiles to the spectra, are 0.37 ± 0.02 Rayleighs, 0.21 ± 0.04 R, and 0.20 ± 0.02 R from MS II A, MS III, and MS IV C respectively. The features around 6563 Å in the MS II A spectrum are due to incomplete cancellation of the geocoronal H α line, which shows large temporal variations.

The high negative velocity of MS VI, combined with an unfavorable LSR velocity correction, places it on the wing of the OH 6553.6 Å line; we can only set an upper limit of 0.4 Rayleighs on emission from this field, and will exclude it from further discussion. We also observed a field, MS II B, located about midway between the MS II A and MS III fields, which is on the Stream but not on a cloud leading edge. This spectrum is shown in Figure 3(a); the “bump” at 6560.25 Å is only marginally significant, having intensity 0.07 ± 0.02 R, which suggests that the H α emission is strongest on the cloud leading edges.

Our observations around the MS IV concentration allow us to investigate this possibility in more detail. The map of H I surface density in this region (Figure 1 of Cohen 1982) shows a strong wedge-shaped density gradient at 23 $^{\text{h}}42^{\text{m}} -12^{\circ}$, and trailing, fragmented lower-density contours to the northwest, reminiscent of a bow shock or ram pressure stripping. We observed four fields along the Stream, designated A through D. Fields A & B are ahead of the density gradient, C is on the gradient, and D is behind it. The spectra of A, B, & D are presented in Figure 3(b-d), and

the spectrum of C is in Figure 2(c). For these fields, time constraints forced us to use the same set of four sky exposures for all three object fields. The sky subtraction is poorer, leading to an artificial “dropoff” at both ends of the spectrum.

However, this does not affect the conclusion we draw, which is that the emission clearly is weak at points not on the density gradient. Fields A & B have no significant signature of emission, with 2σ upper limits of 0.04 R and 0.06 R. Field D shows marginal evidence for a double-peaked profile; fitting two Voigt profiles to the peaks yields an intensity of 0.09 ± 0.03 R. The emission from the MS IV C field is much stronger (Figure 2(c)), confirming that the emission is associated with the cloud leading edges. The line profile of the emission from MS IV C is broadened and fairly asymmetric, suggesting that the line of sight passes through at least two components at different velocities.

The results of our observations, including $H\alpha$ velocities and intensities, are summarized in Table 1. There are firm detections of $H\alpha$ emission from MS II A, MS III, and MS IV C, with intensity 0.37 ± 0.02 R, 0.21 ± 0.04 R, and 0.20 ± 0.02 R respectively. The fluxes are 2.6, 1.4, and 1.4×10^{-17} erg cm $^{-2}$ sec $^{-1}$ arcsec $^{-2}$. If the Stream gas is at $\sim 10^4$ °K, the emission measures (EM) are 1.0, 0.5, and 0.5 cm $^{-6}$ pc. The EMs imply ionization fractions of $x \sim 0.5$ in the leading edges. On the leading edges, the $H\alpha$ velocities are in good agreement with the H I velocities, and the velocity dispersions are 15 – 30 km s $^{-1}$. There is at best marginal evidence for $H\alpha$ emission on the points not on the leading edges. (These leading edges are defined by the H I maps for MS II, III, and IV, taken from Morras (1985), Mirabel, Cohen & Davies (1979), and Cohen (1982) respectively.)

The $H\alpha$ intensity, velocity, and velocity dispersion are derived from a Voigt profile fitted to the combined spectrum, allowing for a gaussian velocity dispersion convolved with the instrumental Voigt profile of the RFP. They may be affected by non-gaussian velocity substructure such as blending along the line of sight, as illustrated by the MS IV C spectrum; substructure in the line profile has a small effect on the derived intensity, but it can have a large effect on the derived velocity dispersion. We searched for spatial structure in the emission by dividing the images into quadrants and fitting a Voigt profile to each quadrant separately; no significant variations in intensity were seen. The formal errors in the $H\alpha$ velocities yielded by the fit are in all cases less than 5 km s $^{-1}$.

The important results from the observations are: (1) the $H\alpha$ emission is associated with leading edges of the clouds, since the detections are all located on leading edges, and there are no compelling detections on the non-leading edge fields, and (2) the $H\alpha$ intensity does not correlate with the observed H I column density.

For all fields in which we observe significant emission, the $H\alpha$ velocity agrees with the H I velocity (see Table 1). The velocities are sufficiently high that Galactic contamination is implausible. Since we observe emission in several different fields at different wavelengths, we are certain that the emission cannot be a weak atmospheric feature. The sky-subtraction process is

relatively simple, and we have taken care to alternate object-field and sky-field exposures, to avoid temporal variations. We conclude that the observed signatures are genuine $H\alpha$ emission from the Magellanic Stream.

4. Sources of Emission – Contact with coronal gas

The similarity of the $H\alpha$ intensity on the leading edges of MS II, III, and IV motivates us to seek a common cause. We will show that the most likely cause is emission generated as the Stream clouds are heated by kinetic and thermal energy input, presumably caused by the motion of the Stream clouds through a galactic corona of hot ionized gas.

The $H\alpha$ emission could result from collisional ionization caused by some form of mechanical energy input; the most plausible source is contact between the Stream clouds and an lower-density ambient ionized medium. The $H\alpha$ emission could be powered by ram pressure heating as the clouds move through ambient gas in the Galactic halo, or by thermal conduction from hot, ionized gas, or both. Notably, ram pressure sweeping may explain the shapes of the leading edges of the LMC and the Magellanic Stream clouds, and the associated H I density gradients, as suggested by Mathewson *et al.* (1977).

4.1. Ram pressure heating

The tapered shape of the Stream clouds and the H I density gradients on their leading edges suggest that the clouds are moving through lower density ambient gas. If so, the ram pressure from the ambient gas will transfer energy to the Stream clouds, heating their leading faces. This would naturally explain the association of $H\alpha$ emission with leading edges. However, it is difficult to calculate the efficiency of the process in which energy input due to ram pressure is converted to energy output by radiation.

4.1.1. A simple drag model

We can make a crude estimate by assuming that the Stream clouds are subject to a drag force from the lower-density ambient gas. As a simple model, we assume that the cloud does not accrete material from the hot medium, and that the kinetic energy the cloud loses to drag goes into heating the leading face of the cloud.

Approximating the cloud as a solid body moving through the hot gas, we express the drag in the standard form:

$$\frac{dp}{dt} = F_{drag} = -\frac{1}{2}C_D\rho_1Av^2, \quad (1)$$

where C_D is a dimensionless drag coefficient dependent on the cloud shape, $\rho_1 = 1.4m_Hn_H$ is the density of the coronal gas, A is the frontal area of the cloud, and $v = 220 \text{ km s}^{-1}$ is its velocity relative to the corona. If the coronal gas is at the virial temperature of the halo, the Stream clouds are moving through it at approximately the sound speed in the gas. In this transonic regime, the drag is relatively high, and there is not a stand-off shock ahead of the cloud; rather, we expect the coronal gas to transfer momentum to the Stream cloud at or close to its face. Thus the kinetic energy lost by the cloud is likely to be dissipated into its leading face. Taking $C_D = 1$ and assuming the energy is distributed uniformly over the cloud face, the input energy flux Σ_{in} is

$$\Sigma_{in} = \frac{1}{2}\rho_1v^3. \quad (2)$$

We now assume that this energy is all converted to radiation, and consider the case of the MS IV leading face. The flux in H α from the MS IV C field is $\Sigma_{obs} = 6.0 \times 10^{-7} \text{ erg cm}^{-2} \text{ s}^{-1}$. MS IV has a opening angle of $\sim 90^\circ$, so we assume that the emission is enhanced by a factor of 3 due to the depth of the heating zone along our line of sight. Then the ambient gas density required to supply the energy emitted in the H α line *alone* ($\Sigma_{in} = \Sigma_{obs}/3$) is $n_H(\text{H}\alpha) = 1.5 \times 10^{-5} \text{ cm}^{-3}$.

If the Stream gas is at $T \sim 10^4 \text{ K}$, as suggested by its velocity width and the presence of H α , there are 2.2 recombinations per H α photon (Pengelly 1964; Martin 1988). Since an H α photon carries off only one-seventh of the energy of a recombination, and energy must also go into metal emission lines and internal motions in the cloud, the required density of diffuse gas in the halo is on the order of $n_H \sim 10^{-4} \text{ cm}^{-3}$ or greater.

This model involves a chain of assumptions: that the coronal gas exerts drag on the cloud with $C_D \sim 1$; that the drag heats the face of the cloud; and that this heat will be efficiently converted into radiation. The first assumption is justified for a blunt object such as a gas cloud, in the low viscosity regime applicable here (*e.g.* Figure 3.15 of Tritton 1988). The drag acts by increasing the pressure on the leading face of the cloud (*e.g.* Figure 12.9 of Tritton 1988), so that it is reasonable to assume that the kinetic energy lost to drag by the cloud is converted to heat at the face.³ Finally, the H α and H I velocity dispersions indicate that the cloud gas is at $T \sim 10^4 \text{ }^\circ\text{K}$, so it will quickly lose the heat energy to radiation, due to the steepness of the cooling curve above $10^4 \text{ }^\circ\text{K}$.

³Follow-up observations in August 1995, to be reported fully in a later paper, confirm that H α emission of 0.05 – 0.2 R is distributed over the leading face of the MS IV cloud.

The model demonstrates that the drag from coronal gas of density $n_{\text{H}} \sim 10^{-4} \text{ cm}^{-3}$ can generate an energy input to the MS cloud that is of the right order of magnitude to power the observed $\text{H}\alpha$ emission. This is only an order of magnitude estimate, as there are a number of competing factors whose values are uncertain, such as the drag coefficient and the efficiency of conversion of kinetic energy to radiation. Nonetheless, it is significant that the implied coronal density is similar to that inferred by Wang (1992) from observations of the X-ray background.

4.1.2. Instability of the flow

The drag analysis above treats the Stream cloud as a solid object moving through coronal gas. As a first approximation, this is reasonable, since the Stream gas is much denser than the putative corona. However, it is incomplete, since the interface between the cloud and the coronal gas may be unstable. Even if the cloud and the corona are in pressure equilibrium, the flow of the coronal gas past the surface of the cloud may be subject to the Kelvin-Helmholtz instability, which arises at the interface of two fluids with a relative shear velocity.

The Kelvin-Helmholtz instability occurs for all wavelengths λ satisfying

$$\lambda < \lambda_{crit} = \frac{2\pi n_1 n_2 v^2}{g(n_2^2 - n_1^2)}, \quad (3)$$

where $g = GM_c/R_c^2$ is the gravitational acceleration at the surface of the Stream cloud, n_1 and n_2 are the number densities of the hot gas and the cloud, and v is their relative velocity (Chandrasekhar 1961). These formulae apply to incompressible fluids; the incompressible case is a good approximation in all but strongly supersonic motion (Bradshaw 1977). The e -folding timescale for the growth of a perturbation is τ (Chandrasekhar 1961):

$$\tau = \left[\frac{4\pi^2 n_1 n_2 v^2}{\lambda^2 (n_1 + n_2)^2} - \frac{2\pi g (n_2 - n_1)}{\lambda (n_1 + n_2)} \right]^{-1/2}. \quad (4)$$

For the dense cloud at the head of MS IV, we assume its distance to be 50 kpc, obtaining approximate values of $M_c = 2 \times 10^7 M_\odot$, $R_c = 700 \text{ pc}$, and $n_{2\text{H}} = 0.05 \text{ cm}^{-3}$ (Cohen 1982), and assume the cloud velocity is $v = 220 \text{ km s}^{-1}$ and the coronal density $n_{1\text{H}} = 10^{-4} \text{ cm}^{-3}$. This yields a critical wavelength of $\lambda_{crit} = 3.5 \text{ kpc}$. Since this is larger than the size of the dense cloud, and comparable to the width of the entire low-density component of the Stream, the cloud-corona interface is unstable on all relevant length scales.⁴

⁴The instability can be suppressed by a magnetic field of strength $B_{\parallel} > 1 \mu\text{G}$ everywhere parallel to the shear velocity, but this is unlikely in gas of such low density.

Representative timescales for the instability to develop are $\tau_{10} = 1.6 \times 10^5$ yr and $\tau_{1000} = 1.9 \times 10^7$ yr for perturbations of wavelength 10 pc and 1 kpc respectively. These are shorter than the orbital timescale, $\tau_{dyn} = \text{several} \times 10^8$ yr, and therefore the interface between the Stream cloud and the coronal gas will become complex and turbulent. This increases the likelihood that coronal gas can transfer energy to the cloud; it also suggests that the cloud will itself be ram pressure stripped by the corona. The H I observations of the Stream show dense clouds trailed by diffuse H I with a complex distribution (*e.g.* Figure 1 of Cohen 1982), suggesting that the clouds are indeed being stripped by ram pressure. Since the cloud sizes are a few kpc, the stripping will occur over timescales $\sim \tau_{1000}$. This may contribute to the observed decrease in peak H I column density along the Stream from MS I to MS VI.

4.2. Thermal conduction

If the clouds of the Magellanic Stream are surrounded by coronal ambient gas, it is presumably ionized and quite hot, at the virial temperature of the Galactic halo. Thermal conduction at the cloud–corona interface will heat the cloud and produce an ionized zone at the surface, in which recombination and H α emission can occur.

If the clouds of the Magellanic Stream are in contact with a hot corona of $T = 1.7 \times 10^6$ °K, the virial temperature of the Galactic halo (Fall & Rees 1985), and the corona has density $n_H = 10^{-4}$ cm $^{-3}$, motivated by Wang (1992), and the subclouds observed have $R \sim 1$ kpc, then the clouds will evaporate, and the evaporation will be unsaturated (McKee & Cowie 1977). The emission measure expected from a conduction front in an evaporating cloud is calculated in §IIIb of McKee & Cowie (1977); ignoring photoionization of the skin of the cloud, the EM is less than $n_H^2 R$, and if photoionization drives the ionization front, the EM is $\sim 18n_H^2 R = 2 \times 10^{-4}$ cm $^{-6}$ pc. This is far below the observed EMs of 0.5 to 1 cm $^{-6}$ pc, even if the lines of sight pass through multiple conduction fronts, or if the interface between the cloud and corona is augmented by the Kelvin-Helmholtz instability described above.

Additionally, thermal conduction does not explain the association of H α with leading edges. Radiation from an ionized cloud–corona interface should be uniform across the clouds, or perhaps exhibit a correlation with gas density, since recombinations could occur more easily in regions of higher density. However, the observations show no trend of H α with H I column density. Hence, although thermal conduction may contribute, it is not the primary cause of the observed H α .

5. Other Sources of Emission

We now consider and rule out other potential sources of emission which do not invoke the presence of Galactic coronal gas.

5.1. Relic recombination

Could the H α be a relic of a transient ionization phenomenon that occurred as the clouds of the Stream were detached from the Magellanic Clouds? This is implausible, since the Stream, as observed in H I, does join onto the Clouds. Nevertheless, we can rule this out firmly by comparing the orbital timescale to the recombination timescale.

Consider the case of MS IV, which trails the Magellanic Clouds by $\sim 70^\circ$ on the sky. A simple lower limit to the time since MS IV separated from the Clouds is the time t_{min} it takes the Clouds to move 70° of arc in their orbit. Since MS IV presumably retains some transverse velocity this should be an underestimate. The galactocentric transverse velocity of the LMC is $215 \pm 48 \text{ km s}^{-1}$ (Jones *et al.* 1994), and its distance is $\sim 50 \text{ kpc}$, giving $t_{min} \sim 2.8 \times 10^8 \text{ yr}$.

If the ionization was a single event, the recombination rate was probably greater in the past, so it is conservative to assume a constant rate equal to that implied by the observations, $\eta_{rec} = 4.4 \times 10^5 \text{ cm}^{-2} \text{ s}^{-1}$. From the observations of Cohen (1982), the clump at the leading edge of MS IV has an angular radius $\theta \gtrsim 1^\circ$. This suggests that constant recombination since a single drastic ionization should produce a mass of H I in MS IV,

$$M_{\text{HI}} > \pi(\theta D)^2 m_p \eta_{rec} t_{min} = 30,000 D^2 M_\odot, \quad (5)$$

where D is the distance to MS IV in kiloparsecs.

The observations of MS III and MS IV by Cohen (1982) detected a total H I mass of $M_{\text{HI}} = 9000 D^2 M_\odot$, of which roughly half belongs to MS IV, a factor of about 6 less than the supposed lower limit. In other words, steady recombination since a single ionization event would produce much more H I than is observed. Comparing the product $\eta_{rec} t_{min} = 3.8 \times 10^{21} \text{ cm}^{-2}$ (expected column density) to Cohen’s observed peak column density on MS IV, $N_{\text{HI}} = 1.3 \times 10^{20} \text{ cm}^{-2}$, yields a similar conclusion. The present-day H α emission is too strong to be a remnant of a single ionization event.

5.2. Photoionization

We now rule out present-day sources of photoionization. The H I column densities in all observed fields are optically thick to ionizing radiation, so any uniform ionizing flux should

produce ionization rates and H α emission which are roughly constant from field to field; this is not observed. (This also excludes other uniform sources such as cosmic rays.) Additionally, the only plausible sources of a uniform ionizing background are the extragalactic radiation field, and any ionizing flux emergent from the Galactic disk. Upper limits on the ionizing flux from Fabry-Perot H α observations show that these sources cannot produce H α flux as high as observed on the Stream (Kutyrev & Reynolds 1989, Songaila *et al.* 1989, Vogel *et al.* 1994).

The required photoionization rates could be produced by a small number of OB stars, *e.g.* just one star producing 10^{48} photons s^{-1} located ~ 100 pc ($\sim 6'$) away from the observed field. However, such a star in the Stream would produce a luminous H II region, which would be easily detected in surveys such as the H α survey mentioned by Mathewson *et al.* (1979). Additionally it is implausible that such a star, with a lifetime less than a few $\times 10^7$ years, could be associated with the Stream, much less that several stars or groups should be fortuitously located to produce similar H α intensities on MS II, III, and IV. This coincidence of intensities would be required for any discrete sources of photoionization. Hence photoionization is ruled out as a cause of the H α emission.

6. Conclusions

The H α emission from the leading edges of MS II, MS III, and MS IV is best explained by ram pressure heating from a surrounding medium of low-density gas; although there are several unknown factors in this process, it is the only candidate which can produce the right order of magnitude of energy output.

This gas is likely to be at the virial temperature of the Galactic halo, $\sim 1.7 \times 10^6$ °K, and nearly completely ionized, undetectable except in X-rays. The similarity of the H α fluxes from MS II, III, and IV shows that this ambient medium is distributed over large scales. This suggests that the Stream is moving through a Galactic corona of hot, ionized gas of density $n_H \sim 10^{-4}$ cm^{-3} .

How far does this corona extend? Although the distance of the Stream is unknown, MS I is joined to the H I envelope which surrounds the Magellanic Clouds, and is thus 50 to 60 kpc distant. The distance of MS II must be similar; the distance of MS IV is less certain, but from 30 to 60 kpc in most models. Thus these observations imply a coronal density $n_H \sim 10^{-4}$ cm^{-3} at ~ 50 kpc above the galactic plane, since the Stream clouds detected are at $b = -70^\circ$ to -80° . The corona is presumably of equal or greater extent in the plane of the Galaxy.

This implies that the Galaxy has a very large *baryonic*, gaseous extent, much larger than previously known; studies of gas in the Galactic halo have shown high- z gas extending out of the disk, but probe only to scale heights of several kpc (*e.g.* Savage & de Boer 1979, Reynolds 1991, Danly 1992, Albert *et al.* 1994), while studies of the X-ray background have suggested a gaseous corona (*e.g.* Wang 1992), but cannot give distance information. This extended corona is a

significant phase of the interstellar medium of the Galaxy. Assuming it is distributed smoothly, a rough lower limit on its mass is $2 \times 10^9 M_{\odot}$, the mass of a sphere of primordial gas with constant density $n_{\text{H}} = 10^{-4} \text{ cm}^{-3}$ and radius 50 kpc.

The most immediate consequence of such an extensive gaseous corona is to suggest that ram pressure stripping is significant in the origin of the Magellanic Stream. The density implied for the coronal gas is very similar to that assumed in the model of Meurer *et al.* (1985), for example; however, their best model requires an extremely high drag coefficient C_D , implausible given the present $\text{H}\alpha$ measurements; the model of Moore & Davis (1994) overcomes this difficulty, but requires the additional presence of an extended ionized gaseous disk.

Secondly, this coronal gas is in rough pressure equilibrium with the Stream clouds, if the clouds are at $T \sim 10^4 \text{ }^{\circ}\text{K}$. This pressure confinement is necessary to stabilize the Stream clouds (Mirabel, Cohen & Davies 1979). It is pleasing to note that this echoes the cloud-confinement argument which led Spitzer (1956) to propose the presence of hot gas in the halo of the Galaxy.

The present result also provides evidence supporting the conjecture of Bahcall & Spitzer (1969) that normal galaxies have large gaseous halos, which they invoked to account for QSO absorption lines, presumed to arise in low column-density neutral systems within the halos. Recent work (Lanzetta *et al.* 1994) suggests that many low-redshift absorption systems are indeed associated with galaxies, which requires normal galaxies to have a gaseous extent of $\sim 160h^{-1}$ kpc. This is compatible with the coronal density at 50 kpc suggested in this paper (Mo 1994).

Additionally, it has long been known that a hot ionized corona could contribute to the observed soft X-ray background (*e.g.* Silk 1974, McCammon *et al.* 1983). The detection of an X-ray shadow due to the Draco Nebula shows that there is soft X-ray emitting gas outside the Local Bubble, but gives only a lower limit of ~ 600 pc for the distance (Snowden *et al.* 1991, Burrows & Mendenhall 1991). These results also suggest that any corona may be patchy or not smoothly distributed. Wang (1992) concludes that a corona of density $n \sim 10^{-4} \text{ cm}^{-3}$ at 50 kpc is consistent with the X-ray background.

In conclusion, we have detected $\text{H}\alpha$ emission from several clouds of the Magellanic Stream, of EM $0.5 - 1 \text{ cm}^{-6} \text{ pc}$. The emission is best explained by ram pressure heating of the Stream as it moves through hot ionized coronal gas, of density $n_{\text{H}} \sim 10^{-4} \text{ cm}^{-3}$ at a Galactic radius $R \sim 50$ kpc. This implies that the Galaxy has a very large baryonic, gaseous extent, in accord with recent studies of low-redshift QSO absorption lines, and supports ram-pressure models for the origins of the Magellanic Stream. Further observations and modeling of the Stream may provide an unprecedented opportunity to probe gas in the outer Galactic halo.

It is a pleasure to thank the CTIO staff for their customary excellent support, particularly Luis Gonzalez for his assistance at the telescope. We thank the referee, Knox Long, for an important correction regarding shocks. BW thanks Povilas Palunas and Karl Gebhardt for advice and encouragement. We are also grateful to Illimani, God of the Andes, for propitious

weather. The RFP was developed with support from Rutgers University and the NSF, under grant AST-8319344.

REFERENCES

- Acker, A., Ochsenbein, F., Stenholm, B., Tyllenda, K., Marcout, J., & Schohn, C. 1993, *Strasbourg-ESO Catalog of Galactic Planetary Nebulae*, (Garching: ESO).
- Albert, C.E., Welsh, B.Y., & Danly, L. 1994, *Ap. J.* 437, 204.
- Bahcall, J.N., & Spitzer, L. 1969, *Ap. J. Lett.* 156, L63.
- Beers, T.C., Flynn, K., & Gebhardt, K. 1990, *A.J.* 100, 32.
- Bradshaw, P. 1977, *Ann. Rev. Fluid Mech.* 9, 33.
- Bregman, J.N. 1979, *Ap. J.* 229, 514.
- Brück, M.T., & Hawkins, M.R.S. 1983, *A. & A.* 124, 216.
- Burrows, D.N., & Mendenhall, J.A. 1991, *Nature* 351, 629.
- Chandrasekhar, S. 1961, *Hydrodynamic and Hydromagnetic Stability*, (Oxford: Clarendon Press).
- Cleveland, W., & McGill, R. 1984, *J. Am. Stat. Assoc.* 79, 807.
- Cohen, R.J. 1982, *MNRAS* 199, 281.
- Danly, L. 1992, *PASP* 104, 819.
- Fall, S.M., & Rees, M.J. 1985, *Ap.J.* 298, 18.
- Gardiner, L.T., Sawa, T., & Fujimoto, M. 1994, *MNRAS* 266, 567.
- Kutyrev, A.S., & Reynolds, R.J. 1989, *Ap. J. Lett.* 344, L9.
- Jones, B.F., Klemola, A.R., & Lin, D.N.C. 1994, *A.J.* 107, 1333.
- Lanzetta, K., Bowen, D.V., Tytler, D., & Webb, J.K. 1995, *Ap. J.* 442, 538.
- Lin, D.N.C., Jones, B.F., & Klemola, A.R. 1995, *Ap. J.* 439, 652.
- Lin, D.N.C., & Lynden-Bell, D. 1977, *MNRAS* 181, 59.
- Lu, L., Savage, B.D., & Sembach, K.R. 1994, *Ap. J. Lett.* 437, L119.
- Martin, P.C. 1988, *Ap. J. Suppl.* 66, 125.
- Mathewson, D.S., Cleary, M.N., & Murray, J.D. 1974, *Ap. J.* 190, 291.
- Mathewson, D.S., Ford, V.L., Schwarz, M.P., & Murray, J.D. 1979, in *The Large Scale Characteristics of the Galaxy*, IAU Symp. 84, ed. W.B. Burton, (Dordrecht: Reidel), p. 547.
- Mathewson, D.S., Schwarz, M.P., & Murray, J.D. 1977, *Ap. J. Lett.* 217, L5.
- McCammon, D., Burrows, D.N., Sanders, W.T., & Kraushaar, W.L. 1983, *Ap.J.* 269, 107

- McKee, C.F., & Cowie, L.L. 1977, *Ap. J.* 215, 213.
- Meurer, G.R., Bicknell, G.V., & Gingold, R.A. 1985, *Proc. A.S. Aust.* 6, 195.
- Mirabel, I.F., Cohen, R.J., & Davies, R.D. 1979, *MNRAS* 186, 433.
- Mo, H.J. 1994, *MNRAS* 269, L49.
- Moore, B., & Davis, M. 1994, *MNRAS* 270, 209.
- Morras, R. 1985, *A.J.* 90, 1801.
- Murai, T., & Fujimoto, M. 1980, *PASJ* 32, 581.
- Osterbrock, D.E., & Martel, A. 1992, *PASP* 104, 76.
- Pengelly, R.M. 1964, *MNRAS* 127, 145.
- Recillas-Cruz, E. 1982, *MNRAS* 201, 473.
- Reynolds, R.J. 1991, in *The Interstellar Disk-Halo Connection in Galaxies*, IAU Symp. 144, ed. H. Bloemen, (Dordrecht: Kluwer), p. 67.
- Savage, B.D., & de Boer, K.S. 1979, *Ap. J. Lett.* 230, L77.
- Shuter, W.L.H. 1992, *Ap. J.* 386, 101.
- Silk, J. 1974, *Comments Ap. Space Phys.* 6, 1.
- Snowden, S.L., Mebold, U., Hirth, W., Herbstmeier, U., & Schmitt, J.H.M. 1991, *Science*, 252, 1529.
- Sofue, Y. 1994, *PASJ* 46, 431.
- Songaila, A. 1981, *Ap. J. Lett.* 243, L19.
- Spitzer, L. 1956, *Ap. J.* 124, 20.
- Tritton, D.J. 1988, *Physical Fluid Dynamics*, (Oxford: Clarendon Press).
- Vogel, S.N., Weymann, R., Rauch, M., & Hamilton, T. 1995, *Ap. J.* 441, 162.
- Wang, Q.D. 1992, *PASP* 104, 812.
- Williams, T.B. 1994, in *Ultraviolet Technology V*, ed. R.E. Huffman and C.G. Stergis, *SPIE Proc.* Vol 2282, 65-75.

Fig. 1.— (a) Spectrum from one 15-minute exposure on the MS II A field. The strong feature at 6563 \AA is geocoronal $H\alpha$; the smaller feature at 6560 \AA is associated with the MS II cloud. The size of the symbols is approximately the size of the error bars.

(b) As (a) but for the corresponding sky field.

(c) The sky-subtracted spectrum; a constant continuum estimated from regions away from the emission has been subtracted. The error bars are shown.

Fig. 2.— Total spectra, with sky and continuum subtracted, for three object fields located at leading edges of H I concentrations in the Stream. The error bars on individual points are omitted for clarity. The solid line is the LOWESS-smoothed fit to the data. The inverted triangles indicate the blueshift of $H\alpha$ expected from the H I velocity given by 21 cm observations.

(a) MS II, field A, on the leading edge of the MS II cloud. The fluctuations around 6563 \AA are residuals from the geocoronal $H\alpha$ line.

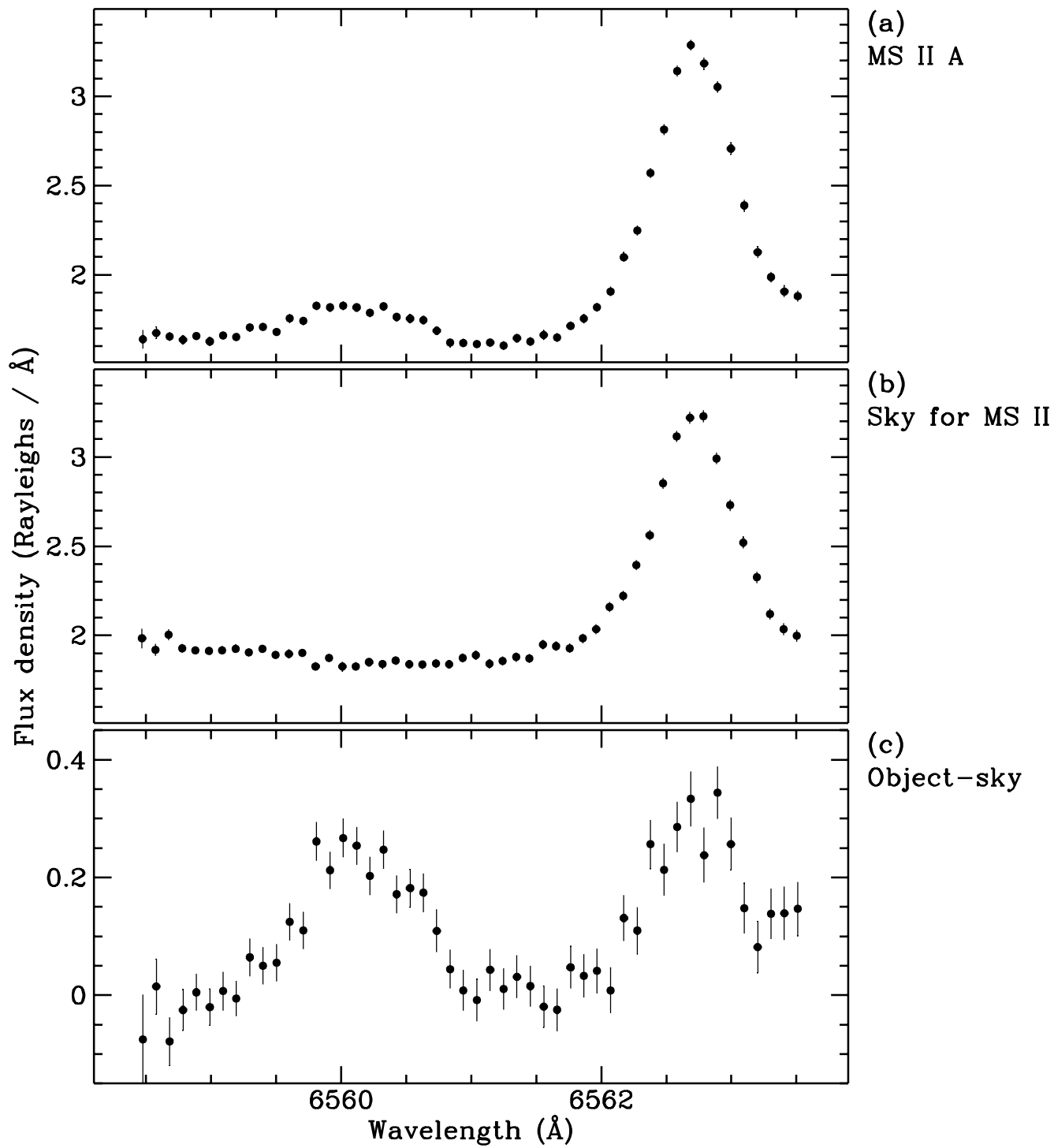
(b) MS III, leading edge.

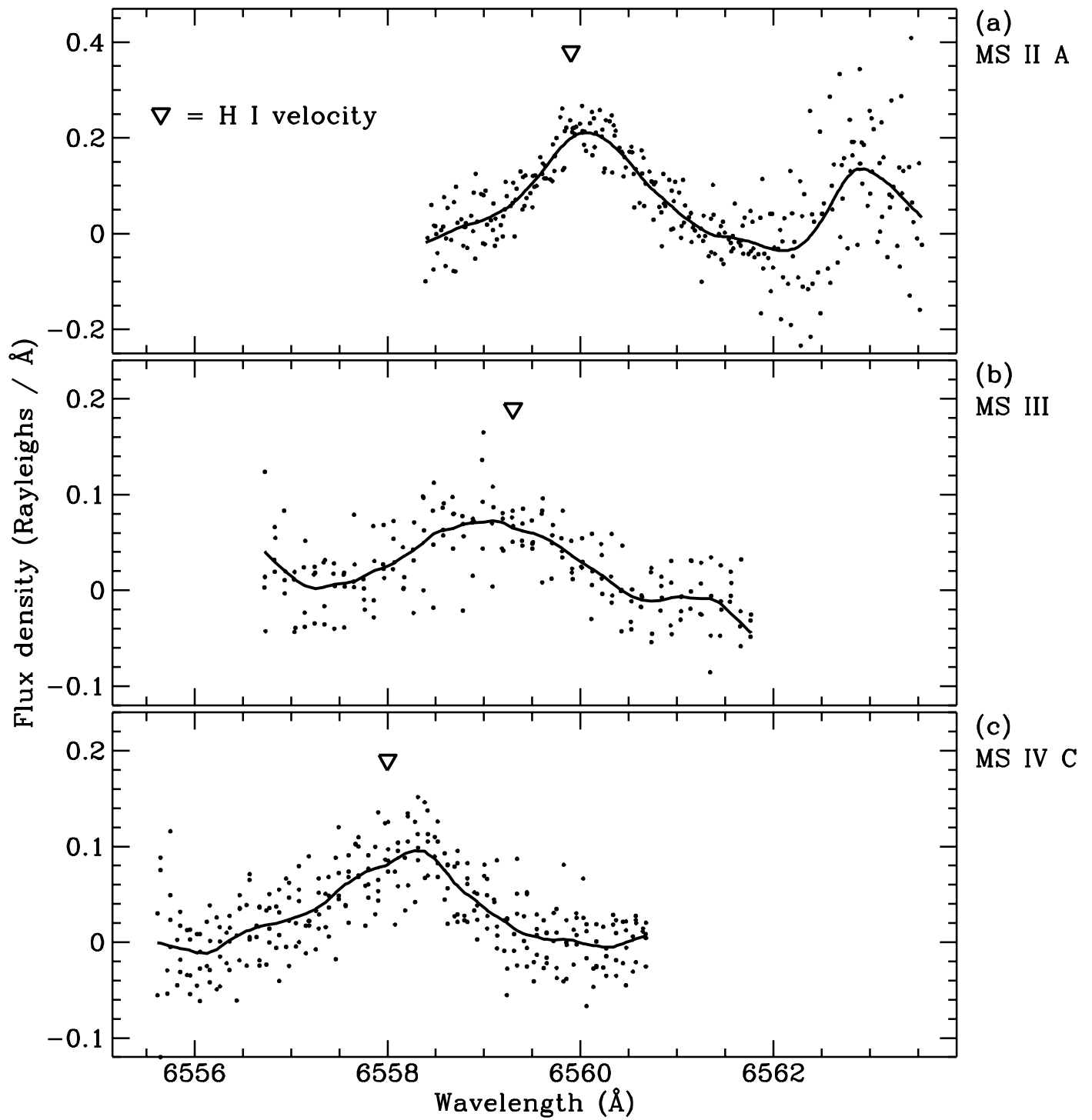
(c) MS IV C, leading edge.

Fig. 3.— Total spectra, with sky and continuum subtracted, for four fields on the Stream, but not on cloud leading edges.

(a) MS II B. Some points near 6563 \AA lie outside the range of the graph, due to large residuals from the geocoronal $H\alpha$ line.

(b-d) MS IV A, MS IV B, and MS IV D.





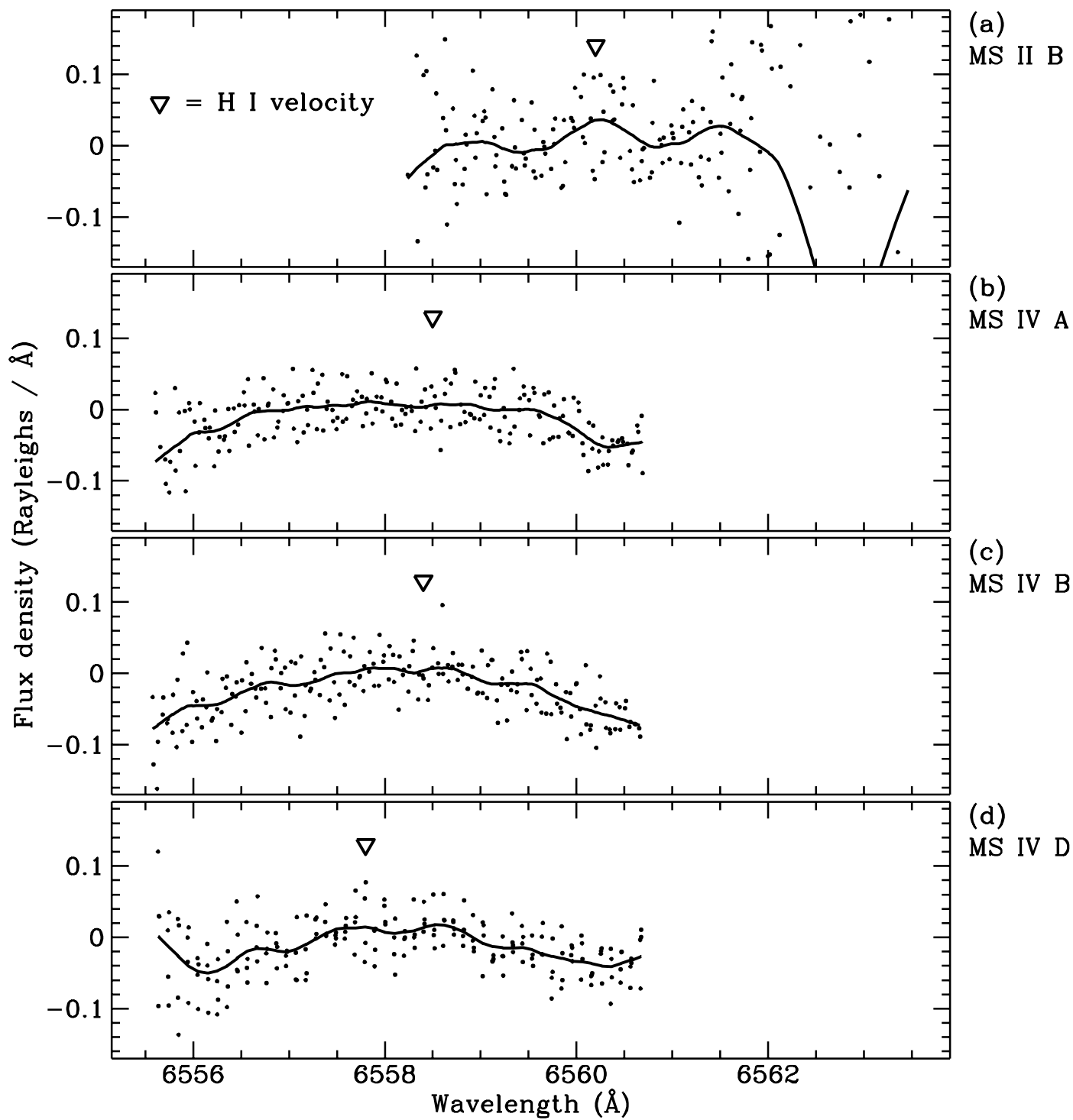


TABLE 1. Results of Observations

Field	Position (1950)		Exposure ^a	Leading	H α Flux	H α V_{LSR}	H I V_{LSR} ^b	H I N_{H} ^b	H α σ
	R.A.	Dec	time	edge?	(Rayleighs)	(km s ⁻¹)	(km s ⁻¹)	(cm ⁻²)	(km s ⁻¹)
MS II A	00:18.0	-35°00'	1.5 hr	yes	0.37 ± 0.02	-120	-130	3 × 10 ¹⁹	15
MS II B	00:20.0	-25°00'	1 hr	no	0.07 ± 0.02	-109	-110	5 × 10 ¹⁹	—
MS III	00:10.5	-20°28'	1 hr	yes	0.21 ± 0.04	-163	-150	5 × 10 ¹⁹	30
MS IV A	23:56.0	-16°00'	1 hr	no	< 0.04 ^c	—	-185	5 × 10 ¹⁹	—
MS IV B	23:46.0	-14°00'	1 hr	no	< 0.06 ^c	—	-190	3 × 10 ¹⁹	—
MS IV C	23:42.0	-12°40'	1.5 hr	yes	0.20 ± 0.02	-199	-205	6 × 10 ¹⁹	24
MS IV D	23:38.0	-11°00'	1 hr	no	0.09 ± 0.03	-183, -220	-215	3 × 10 ¹⁹	—

^aOn-object exposure time.

^bThe H I data are from Morras (1985) for MS II, Mirabel *et al.* (1979) for MS III, and Cohen (1982) for MS IV.

^cThe upper limits are 2 σ .